CrossMark

Use of a DC discharge in a plasma reactor with a rotating ground electrode for production of synthesis gas by partial oxidation of methane

Mohammad Mahdi Moshrefi · Fariborz Rashidi · Hamid Reza Bozorgzadeh

Abstract   A recently designed rotating ground electrode plasma reactor has been used to produce synthesis gas by partial oxidation of methane at room temperature and atmospheric pressure without a catalyst. Experiments were performed to investigate the effects of feed flow rate, feed composition, and the presence of nitrogen in the feed. It was shown that increasing the O_2-to-CH_4 molar ratio reduces conversion of the reagents at low feed flow rates but promotes conversion at high feed flow rates. Increasing the O_2-to-CH_4 molar ratio also results in further methane partial oxidation reactions at high feed flow rates. Use of air instead of pure oxygen increases the conversion of methane and oxygen but reduces selectivity for the main products (H_2 and CO). This reactor can be used to produce a wide variety of H_2-to-CO molar ratios for different applications under stable conditions.

List of symbols

Y_i Mole fraction of components in the feed
Y_o Mole fraction of components in the product
W Number of moles of produced water
C Number of moles of produced carbon
G_i Feed flow rate (mole/min)
G_o Product flow rate (mole/min)

M. M. Moshrefi · F. Rashidi (✉)
Chemical Engineering Department, Amirkabir University of Technology, Tehran, Iran
e-mail: rashidi@aut.ac.ir

H. R. Bozorgzadeh
Research Institute of Petroleum Industry, Tehran, Iran

Introduction

Partial oxidation (POX) is one of the main methods used to produce hydrogen or synthesis gas (syngas) from hydrocarbons. Hydrogen and carbon monoxide are not the only products from partial oxidation of methane and carbon dioxide; water and carbon (soot) are also produced in small amounts. Catalysts are usually used to improve product selectivity (CO and H_2) [1–4]. Song et al. [5] used Ni/Al_2O_3 catalysts for partial oxidation of methane. Methods used for preparation of Ni/Al_2O_3 catalysts included the impregnation method (IM), the sol–gel method (SG), and the modified sol–gel method (MSG). For conversion of methane, selectivity for hydrogen and carbon monoxide over 2 % Ni/Al_2O_3-SG was lower than over 2 % Ni/Al_2O_3-MSG (at 700 °C, gas hourly space velocity 1.0×105 mL/g cat h and atmospheric pressure). Activity of the catalysts was almost constant during 100 h of time on stream (TOS). In catalytic partial oxidation, increasing TOS results in surface hot spot formation, which can lead to an unhealthy catalyst. Navalho et al. [6] studied the partial oxidation of hydrocarbons on a rhodium-based catalyst in a non-adiabatic monolith reactor. They reported that use of the non-adiabatic reactor is an effective way of reducing hot spot formation, because radiative heat loss results in a reduction in the maximum surface temperature compared with the adiabatic reaction at low fuel flow rates, high air-to-fuel equivalence ratios, and for fuels with high power densities. Sulfur poisoning of the catalyst is another concern in catalytic partial oxidation of methane [7, 8]. High reaction temperatures and the need for regeneration of deactivated catalysts are often regarded as the main disadvantages of catalytic partial oxidation of methane. In recent years, plasma reactors have led to a new branch of science in which mechanisms of reactions obey the rules of plasma chemistry. Reformation of hydrocarbons by use of different plasma reactors has been discussed in a vast amount of literature [9–15]. Bromberg et al. [16] investigated partial oxidation of methane by use of a thermal plasma reformer (current approximately 100 A, power approximately 10 kW) and reported specific energy consumption of 40 MJ/kg H_2. Disadvantages of the thermal plasma reformer are high temperature, electrode erosion, and low electrode lifetime. Rafiq et al. [17] produced syngas by partial oxidation of methane in a plasma-assisted gliding arc reactor. They suggested two coupled mechanisms, exothermic oxidative and endothermic reforming reactions, to explain the effect of the O_2-to-CH_4 molar ratio on reactor operations. They also reported the effect of reaction temperature as justification of the increasing conversion of methane with increasing gas hourly space velocity. Sreethawong et al. [18] studied the partial oxidation of methane with air for production of synthesis gas in a multistage gliding arc discharge system and reported optimum conditions of: CH_4-to-O_2 molar ratio 3:1, feed flow rate 150 mL/min, and frequency 300 Hz. They concluded that increasing the O_2-to-CH_4 molar ratio results in increased conversion of the reagents, and suggested the reason was the greater number of O_2 molecules reacting with CH_4 at higher O_2-to-CH_4 molar ratios. Supat et al. [19] investigated the partial oxidation of methane with air in an AC electric gas discharge. They studied the effect of O_2-to-CH_4 molar ratio on conversion of methane and reported increased reagent conversion on increasing O_2-to-CH_4 molar ratio. They suggested higher activation of methane molecules at a

higher O_2-to-CH_4 molar ratio as an explanation. Investigation of the effect of feed flow rate revealed that conversion of regents is reduced by increasing the feed flow rate at an O_2-to-CH_4 molar ratio of 1:3. Fridman et al. [20] designed a gliding arc in tornado plasma reactor in which the flow of feed induces an electrical discharge along the electrodes. At an input temperature of 750 K for feed, conversion of methane and H_2-to-CO molar ratio were 92 % and 2, respectively. They reported an electrical energy cost of 0.06 kW h/m^3. A newly designed plasma reactor with a rotating ground electrode (RGE) was used in this study. The RGE plasma reactor has advantages which are fully explained in reports of our previous studies [21–23]. Partial oxidation of methane by use of the RGE plasma reactor was studied to investigate the effects of feed flow rate at different O_2-to-CH_4 molar ratios and the presence of nitrogen in the feed. In the partial oxidation of methane by DC discharge, soot formation is inevitable. The electrical conductivity of soot ($\sim 10^3$ [24]) is less than that of the ground electrode ($\sim 10^6$), which causes loss of electrical energy and, consequently, because of high accumulation of the carbon between the electrodes, electrical potential energy discharges through the carbon instead of by breaking down the gas medium. Carbon deposition on electrodes, which has a negative effect on discharge stability, has been a concern in many studies [25–27]. A catalyst has been used as a remedy to obtain a stable plasma; ultimately, however, because of excessive accumulation of carbon, the DC discharge became unstable. To overcome this problem, in this study a plasma reactor with a novel design, i.e. with a DC discharge based on a rotating ground electrode, was used. Because the ground electrode rotates it can be easily cleaned, increasing the efficiency of reactor. The most important advantage of electrical discharge by use of a rotating ground electrode is stable discharge without use of a catalyst. Rotation of the ground electrode also results in a longer discharge length, which prevents a high electrical potential drop, i.e., by using an RGE plasma reactor higher breakdown voltage can be achieved.

Experimental

Experimental setup consisted of methane (99.99 % purity) and oxygen (99.99 % purity) cylinders with mass flow controllers (MFC Brooks 5850), mixer (a tubular flask used to obtain homogenous gas mixture), plasma reactor, bubble flow meter, silica gel dryer trap, and gas chromatograph (GC, agilent 6890 N). Reactor feed was supplied from gas cylinders via steel tubing through mass flow controllers. After passage through the mixer it was directed to either the plasma reactor or the bubble flow meter to calibrate the MFCs. Both feed composition and product composition were analyzed by on-line gas chromatography (GC) with flame ionization detection (FID), with which such hydrocarbons as ethane, ethylene, acetylene, propane, propylene, and heavier hydrocarbons were analyzed. A thermal detector was connected to a Haysep Q and N and molecular sieve 139 (MS-139) packed column to enable analysis of such gas components as nitrogen, carbon dioxide, carbon monoxide, hydrogen, and methane. A schematic diagram of the setup is shown in Fig. 1. A high-voltage (12 kV), low current (up to 30 mA), DC transformer was
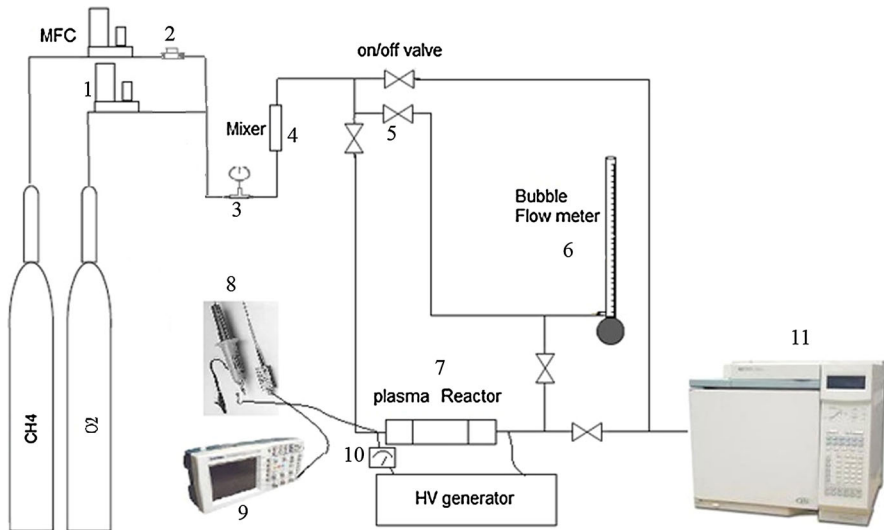
Fig. 1 Schematic diagram of the experimental set-up. *1* MFC, *2* check valve, *3* pressure gauge, *4* mixer, *5* on/off valve, *6* bubble flow meter, *7* plasma reactor, *8* HV probe, *9* oscilloscope, *10* galvanometer, *11* GC

used as the power supply. In all experiments, power consumption was approximately 20 W (electrical voltage was ~ 2 kV and electrical current was ~ 10 mA). The reactor was a quartz tube containing a stainless steel rotating plate, which acted as the ground electrode, and a stainless-steel, high-voltage needle electrode. A DC motor (6,000 rpm) was used to rotate the ground electrode; the high-voltage electrode was fixed. Depending on the amount of soot accumulating on the ground electrode, the speed of the electrode was increased. To obtain a stable voltage waveform, the speed of the ground electrode, which depends on several conditions, including feed flow rate, input electrical power, electrode separation, feed components and composition, diameter of ground electrode, was determined empirically. Electrodes were positioned opposite each other at the same level and 7 mm apart. The outer diameter of the reactor was 30 mm and its length was 150 mm. A schematic diagram of the reactor is shown in Fig. 2. Figure 3 shows a photograph of the electrical discharge through the quartz reactor during a typical experiment. An empty space was provided at the bottom of the reactor to collect carbon aerosols. These were prevented from entering the piping system by use of a ceramic filter. If these carbon aerosols enter the piping system, they prevent flow of gas in the GC sampling loop. In all experiments, product flow rate measured by use of a bubble flow meter was used in material balance calculations. The number of moles of water produced was derived from the oxygen balance (Eq. 1). Results from GC analysis were in agreement with the hydrogen balance (Eq. 2) when the number of moles of water produced was included in calculations. The carbon balance (Eq. 3) was used to determine the number of moles of carbon produced. Conversion of methane and oxygen was defined as in Eqs. (4) and (5). Equations (6) and (7) were used for calculation of selectivity for hydrogen and carbon monoxide on the basis of
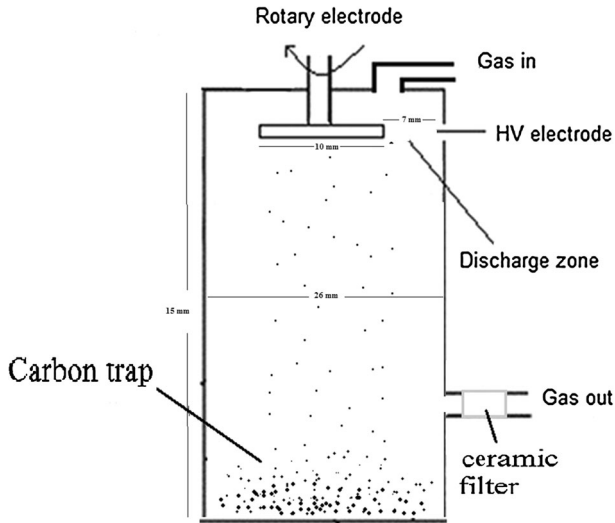
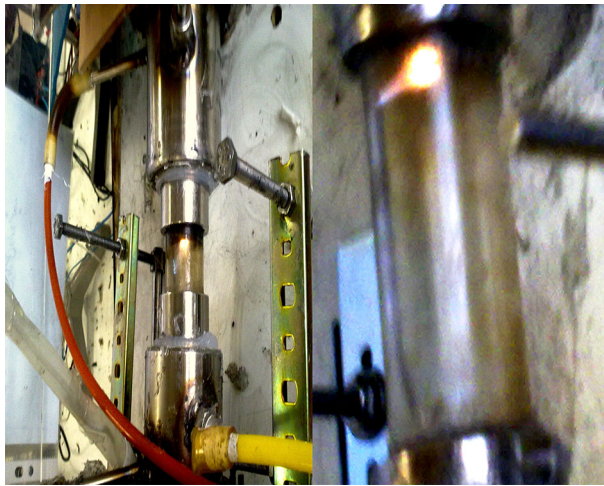**Fig. 2** Schematic diagram of the plasma reactor

Fig. 3 Representative photograph of the electrical discharge through the quartz reactor during a typical experiment

hydrogen and carbon, respectively. Equations (8) and (9) were used to calculate the yields of hydrogen and carbon monoxide. Energy efficiency (η) based on the low heating value (LHV) of hydrogen was defined by Eq. (10) [28]. To make the same comparison, energy efficiency was calculated by use of Eq. (10), and it is assumed that the CO produced is then converted into H_2 by the water gas shift reaction. Experiments were continued until results from two GC analyses of the product were identical. Bubble flow meters were used to calibrate the MFCs, and the flow rate of

the product was measured by use of the same bubble flow meters. Therefore, the error in the feed flow rate and the product flow rate will be the same, say a %. In each experiment, both feed flow rate and product flow rate were analyzed by GC, so the error in the mole fractions of feed and product will be the same, say b %. Use of this technique cancels the errors in the measurements. An example of methane conversion is illustrated by Eq. (11). The same method was used to derive oxygen conversion, product selectivity, etc.

$$W = 2 \times Y_iO_2 \times G_i - (2 \times Y_oO_2 + Y_oCO + 2 \times Y_oCO_2) \times G_o \tag{1}$$

$$4 \times Y_iCH_4 \times G_i - (4 \times Y_oCH_4 + 2 \times Y_oH_2) \times G_o - 2 \times W = 0 \tag{2}$$

$$C = Y_iCH_4 \times G_i - (Y_oCH_4 + Y_oC_O + Y_oCO_2) \times G_o \tag{3}$$

$$\text{Methane conversion} = \frac{\text{moles of methane converted}}{\text{moles of methane introduced}} \times 100 \tag{4}$$

$$\text{Oxygen conversion} = \frac{\text{moles of oxygen converted}}{\text{moles of oxygen introduced}} \times 100 \tag{5}$$

$$\text{Hydrogen selectivity} = \frac{\text{moles of hydrogen formed}}{2 \times \text{moles of methane converted}} \times 100 \tag{6}$$

$$\text{Carbon monoxide selectivity} = \frac{\text{moles of carbon monoxide formed}}{\text{moles of methane converted}} \times 100 \tag{7}$$

$$\text{Hydrogen yield} = \text{methane conversion} \times \text{hydrogen selectiviy} \tag{8}$$

$$\text{Carbon monoxide yield} = \text{methane conversion} \times \text{carbon monoxide selectivity} \tag{9}$$

$$\eta = \frac{(H_2 + CO)_{\text{produced}} \times LHV(H_2)}{\text{Input plasma energy} + (CH_4)_{\text{introduced}} \times LHV(CH)_4} \tag{10}$$
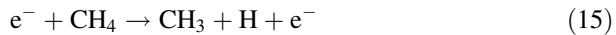
$$\frac{(1 \pm a)(1 \pm b)Gin \times yinCH_4 - (1 \pm a)(1 \pm b)Gout \times youtCH_4}{(1 \pm a)(1 \pm b)Gin \times yinCH_4} = \frac{Gin \times yinCH_4 - Gout \times youtCH_4}{Gin \times yinCH_4} \tag{11}$$

Results and discussion

Proposed reactions in the reactor

Oxidation of methane is highly exothermic and proceeds via a partial oxidation reaction at high temperatures, i.e., increasing the temperature results in further partial oxidation of the methane. Therefore, the reactor temperature has a large effect on the process. During the start-up period, the reactor temperature is

increased, and therefore affects operation of the reactor. In the reaction zone, numerous reactions occur. These reactions may be categorized into different groups comprising (a) electron collisions and (b) chemical reactions; a few of these are listed as follows [24]: (a-1) dissociative attachment, e.g. Eq. (12); (a-2) attachment, e.g. Eq. (13); (a-3) dissociation, e.g. Eqs. (14) and (15).

$$e^- + O_2 \rightarrow 2O + e^- \rightarrow O^- + O \tag{12}$$

$$e^- + O_2 \rightarrow O_2^- \tag{13}$$

$$e^- + O_2 \rightarrow 2O + e^- \tag{14}$$

$$e^- + CH_4 \rightarrow CH_3 + H + e^- \tag{15}$$
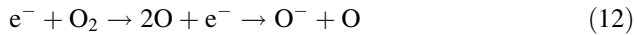
Chemical reactions can be categorized on the basis of the compounds produced, for example chemical reactions which lead to H_2 formation (b-1), e.g. Eqs. (16) and (17), formation of heavier hydrocarbons (b-2), e.g. Eqs. (18) and (19), and formation of CO_x (b-3), e.g. Eqs. (20) and (21).

$$H + H \rightarrow H_2 \tag{16}$$

$$CH_4 \rightarrow C + 2H_2 \tag{17}$$

$$CH_3 + CH_3 \rightarrow C_2H_6 \tag{18}$$

$$CH_2 + CH_2 \rightarrow C_2H_4 \tag{19}$$

$$HCO + O \rightarrow H + CO_2 \tag{20}$$

$$OH + CO \rightarrow H + CO_2 \tag{21}$$

The GC analysis showed that the main products were hydrogen and carbon monoxide. Very small amounts of carbon dioxide and C_2 hydrocarbons were also present. The amount of C_2 hydrocarbons was approximately 0.003 molar ratio at low O_2-to-CH_4 molar ratio, tending to zero at higher molar ratios. C_2 hydrocarbons were ignored in the calculations. At O_2-to-CH_4 = 0.2 molar ratio, the mole fraction of CO_2 produced was approximately 0.002, which increased to 0.006 at O_2-to-CH_4 = 0.5 molar ratio. Although the bulk temperature of the reactor is low, the electron temperature is high in the discharge zone. Therefore, low CO_2 concentrations could be expected on the basis of thermodynamic equilibrium at high temperature, i.e., reaction between produced CO_2 and H_2O to form syngas. If this were so, however, the amount of H_2O in the product should be as low as the amount of CO_2, which does not agree with the results obtained. Alternatively, the low concentration of CO_2 produced may be explained on the basis of plasma chemistry reactions. The O_2-to-CH_4 molar ratio in the feed was low. Radicals formed by electrons colliding with molecules initiated reactions. Hydrogen atoms compete with carbon atoms to reduce the oxygen in the system. If we postulate that when electrons collide with methane molecules all the bonds of methane are broken into hydrogen and carbon, the ratio of hydrogen atoms to carbon atoms will be four, and

there will be a greater tendency to form H_2O, because of the high concentration of hydrogen atoms or hydrogen molecules in the reaction zone. The concentration of remaining oxygen atoms will be so low that complete oxidation of carbon will not occur. Rafiq et al. [17], in a thermodynamic equilibrium study, draw attention to a well known two-stage process for partial oxidation of methane with a short resident time in which H_2O production is high compared with CO_2 production. It was observed that the color of indicating silica gel changed from blue to red, indicating water is being produced. Also at a low O_2-to-CH_4 molar ratio, soot can be seen quite clearly. With regard to this explanation and results from GC analysis, the products are hydrogen, carbon monoxide, water, and carbon. Although there are many possible elementary reactions in the methane partial oxidation system, the number of global reactions that may occur is not so high [29]. It is, therefore, suggested that the main reactions in the reactor are those represented by Eqs. (22)–(24).

$$CH_4 \rightarrow C + 2H_2 \tag{22}$$

$$CH_4 + 1/2O_2 \rightarrow CO + 2H_2 \tag{23}$$

$$2H_2 + O_2 \rightarrow 2H_2O \tag{24}$$
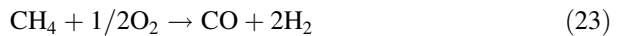
Equations (22)–(24) are summaries of all the reactions which produce hydrogen, carbon monoxide, carbon, and water. In fact, these global reactions (Eqs. 22–24) are sums of hundreds of reactions leading to production of carbon, water, and syngas which may happen in the reaction zone.

Effect of feed flow rate and feed composition on reagent conversion

Two reaction mechanisms, thermal activation and electron collisions, can occur in plasma reactors; these produce ions, dissociated molecules, and excited molecules [30]. In this study, feed entered the reactor at room temperature. The reactor was the cold-plasma type which is not in thermodynamic equilibrium, i.e., the reaction zone contained ions and neutral species at a much lower temperature than the electrons. The bulk temperature of the reactor was therefore low, and the second mechanism was dominant. Condensed water on the reactor wall beyond the discharge zone suggests low bulk temperature. It should be noted, however, that active species are produced by electron collisions followed by methane partial oxidation reactions. In fact, the reactor was affected by two events: production of active species and further methane partial oxidation reactions that followed. The timescale in plasma reactors typically ranges from nanoseconds to microseconds [25]. Theoretically, increasing the feed flow rate is expected to result in a decrease in residence time, and therefore conversion of reagents will decrease, because of the molar balance of the equation; however, this expected trend was not seen for conversion of the reagents at some of the O_2-to-CH_4 molar ratios, as shown in Fig. 4. It should be noted that this affected both production of byproducts and product selectivity. In the following discussion we try to explain this complex behavior. Figure 4 shows that conversion decreases at a low feed flow rate and on increasing the O_2-to-CH_4 molar ratio; however, the slope of this descending trend reduces as feed flow rate increases. When the O_2-to-

Fig. 4 Effect of feed flow rate on conversion of reagents at different compositions: **a** methane conversion, **b** oxygen conversion
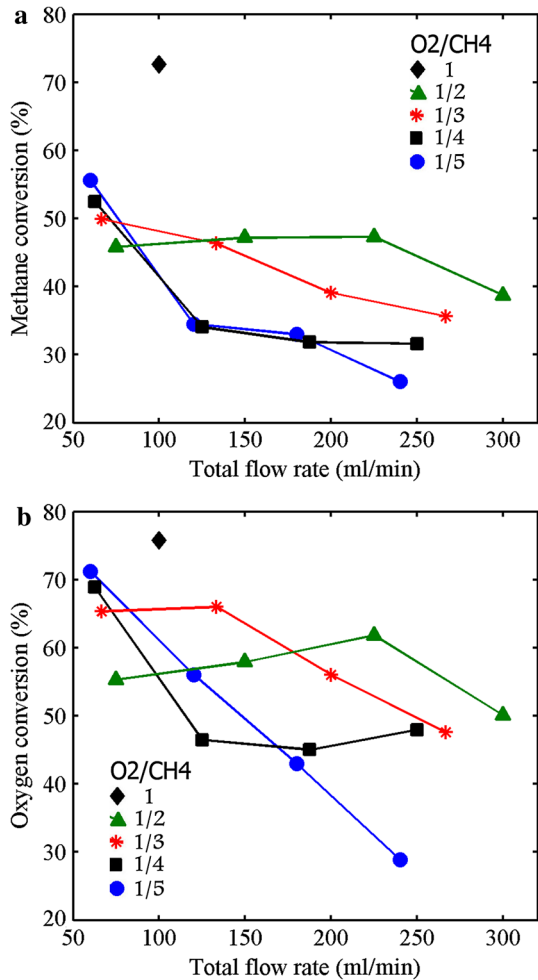
CH_4 molar ratio is increased, a point is reached when, by increasing the feed flow rate, conversion of reagents starts to increase. The aforementioned behavior occurs earlier, i.e., at a lower feed flow rate for a higher O_2-to-CH_4 molar ratio. The reason is further continuation of methane partial oxidation reactions, i.e., increasing both the O_2-to-CH_4 molar ratio and the feed flow rate results in further continuation of the methane partial oxidation reactions. On increasing the feed flow rate, the temperature of the reactor increased [17], and as a result of the increase in the O_2-to-CH_4 molar ratio, the reaction represented by Eq. (23) was promoted.

Effect of feed flow rate and feed composition on selectivity for the main products and on formation of byproducts

The other issue of concern with regard to reactor operation is selectivity for products. Theoretically, feed flow rate is not a thermodynamic quantity, and for a

Fig. 5 Effect of feed flow rate on product selectivity at different compositions: **a** hydrogen selectivity, **b** carbon monoxide selectivity
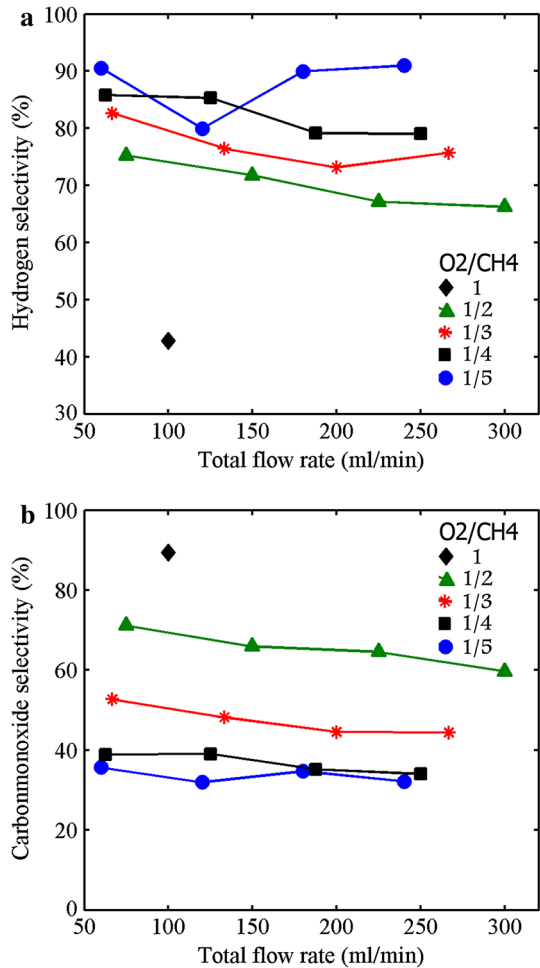

given thermodynamic state reactions mechanisms will not be affected by feed flow rate unless temperature change is significant. Figure 5 shows dependence of selectivity for hydrogen and carbon monoxide on feed flow rate, which suggests that selectivity for products is rather uniform with regard to feed flow rate, i.e., increasing the feed flow rate affects all product components in the same manner. This result has also been obtained in other numerical and experimental studies [17, 29] in which feed flow rate affected reactor operation not because of feed flow rate itself but because of temperature changes which result from changes of feed flow rate. Increasing the O_2-to-CH_4 molar ratio reduces selectivity for hydrogen but increases selectivity for carbon monoxide. The formation of byproducts (water and carbon) explains the above-described behavior. Figure 6 shows the amount of water and carbon produced. On increasing the O_2-to-CH_4 molar ratio, the probability of existence of atomic oxygen increases; therefore, oxidation of hydrogen and carbon

Fig. 6 Effect of feed flow rate on formation of byproducts at different compositions: **a** carbon formation, **b** water formation
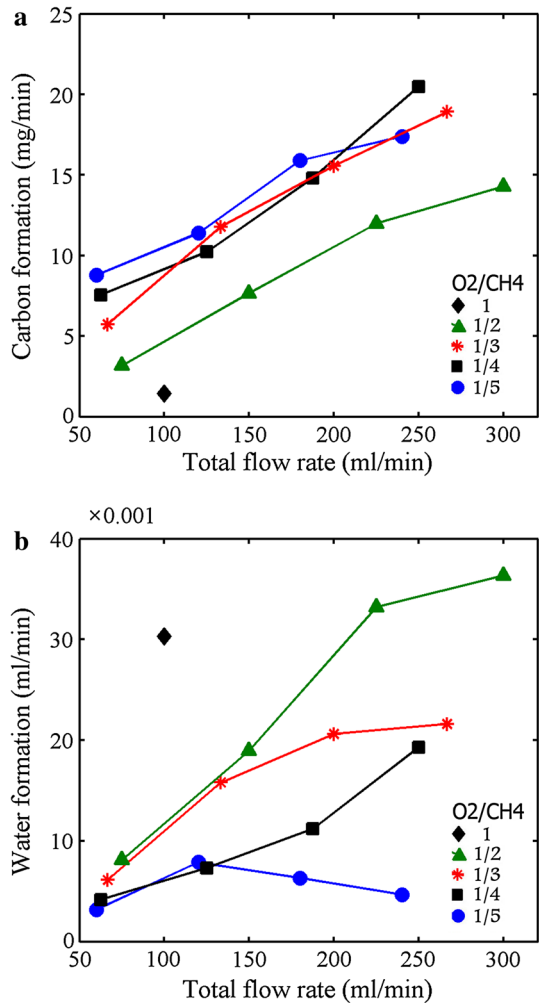

is promoted, i.e., selectivity for hydrogen decreases and selectivity for carbon monoxide increases. Selectivity for carbon monoxide will be less than 100 % because of soot formation; however, increasing the O_2-to-CH_4 molar ratio promotes the oxidation of carbon, and therefore the selectivity for carbon monoxide increases. Theoretically, at higher O_2-to-CH_4 molar ratios complete oxidation proceeds and results in CO_2 production; in this study, however, CO and H_2O are the main products because of the plasma chemistry mechanism of the reactions. Modeling and simulation study [29] of plasma-assisted methane partial oxidation revealed an increase in both CO_2 and H_2O production at high O_2-to-CH_4 molar ratio; the increase of H_2O was, however, much greater than that of CO_2. A kinetic study by Sun et al. [31] suggests a major path for O_2 consumption is production of OH and H radicals by low-temperature plasma partial oxidation. Another kinetic study by

Fig. 7 Effect of feed flow rate on H_2-to-CO molar ratio for different compositions
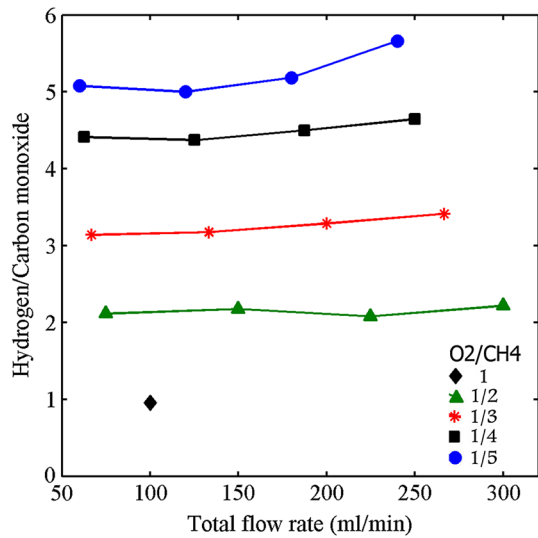
Deminskii et al. [32] confirmed experimental data. They proposed the branched-chain oxidation mechanism at low temperatures in which no branches lead to the CO_2 production. Figure 7 shows the H_2-to-CO molar ratio trend, which is almost independent of feed flow rate but decreases when the O_2-to-CH_4 molar ratio increases, because of the trend of hydrogen and carbon monoxide selectivity explained above. Figures 8 and 9 show, respectively, the dependence on feed flow rate at different compositions of hydrogen concentration and flow rate, and of carbon monoxide concentration and flow rate. These figures indicate that increasing the feed flow rate will cause both H_2 and CO flow rates to increase, whereas there is a descending trend in concentration when feed flow rate is increased. Note that product concentrations were calculated on a dry basis, and as feed flow rate is increased more water is formed. Therefore, the real slopes of CO and H_2 concentrations versus feed flow rate are steeper than in Figs. 8 and 9, i.e., on increasing feed flow rate syngas production increases, but there are some concerns regarding syngas separation. As already explained, H_2O formation will increase when both O_2-to-CH_4 molar ratio and feed flow rate increase. As a result of the increasing amount of H_2O produced, the gaseous phase will become enriched with H_2O and, therefore, the electrical discharge will be unstable because of the high electronegativity of water. This caused some fluctuations in reactor operation, hence repeating the experiments did not give uniform results. As an example, Fig. 10 shows repeatability of results for conversion of CH_4 and O_2 in eight experiments. These fluctuations increased dramatically at a higher O_2-to-CH_4 molar ratio, so that when the O_2-to-CH_4 molar ratio = 1 we were able to obtain only one experimental point for a feed flow rate of 100 mL/min. Note that when O_2-to-CH_4 molar ratios and feed flow rates are low to medium, there is no such problem with repeatability of experiments, as shown in Fig. 10.

Fig. 8 Effect of feed flow rate on hydrogen concentration and flow rate for different compositions: **a** hydrogen concentration, **b** hydrogen flow rate
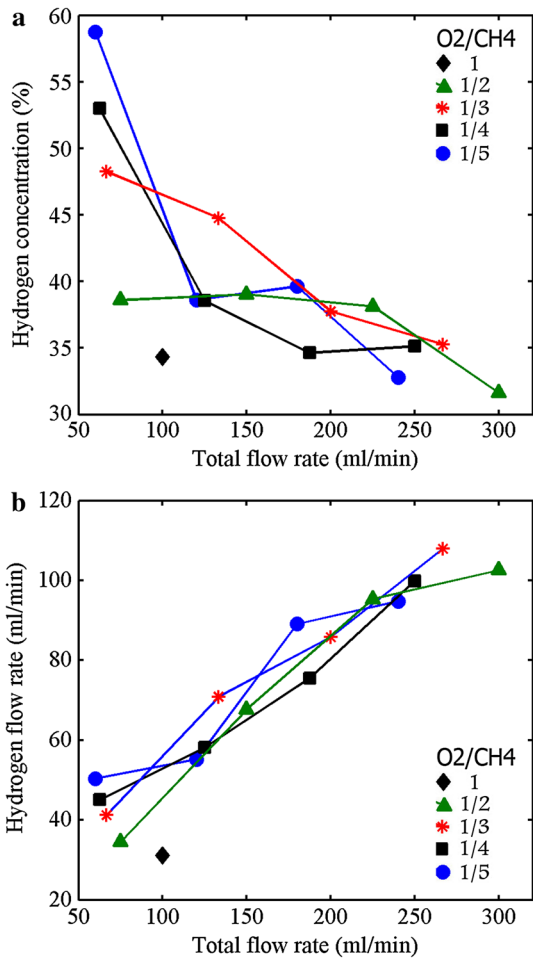
Yield of products and overall review of rotating ground electrode plasma reactor

Table 1 shows an overview of reactor operation with regard to yield of hydrogen and carbon monoxide, stoichiometry of the reaction for each experiment, etc. Increasing the feed flow rate reduces the yield of hydrogen and carbon monoxide at constant feed composition, because of a decrease in the conversion of methane. Increasing the O_2-to-CH_4 molar ratio reduces the yield of hydrogen, because of an increase in the amount of H_2O produced, numerical values for which have been reported elsewhere [29], but increases the yield of carbon monoxide, because of a decrease in deposited carbon. In Table 1, α and β are the percentages of methane which reacts via Eqs. (22) and (23), respectively, and γ is the percentage of hydrogen produced which is converted to water. The overall stoichiometry of the reactions represented by Eqs. (22)–(24), which are based on our experimental results, are given in the last column of Table 1. They indicate how many moles of

Fig. 9 Effect of feed flow rate on carbon monoxide concentration and flow rate for different compositions: **a** carbon monoxide concentration, **b** carbon monoxide flow rate
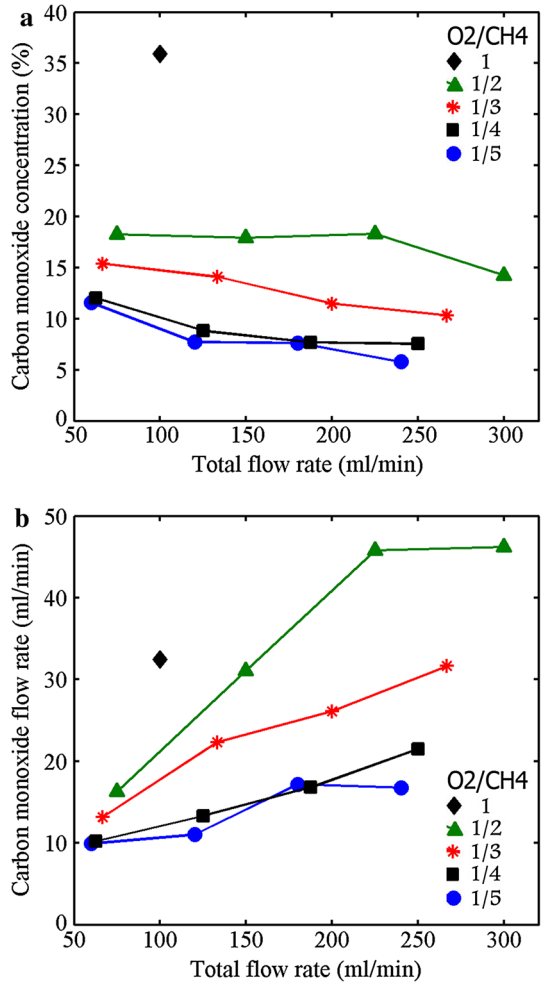
O_2 react with one mole of CH_4 and how many moles of C, CO, H_2, and H_2O are produced from one mole of methane for each feed flow rate and composition. The product and feed flow rates given in Table 1 result in different numbers of moles of gas during the reaction. The volume of the reaction zone consists of:

1. the volume in which energetic electrons collide with reactants; and
2. the subsequent volume in which the produced radicals react.

Neither of these is known, i.e., although feed and product flow rates and reactor volume are known, it is not possible to evaluate the real residence time.

Energy efficiency, energy cost, and specific energy density

Energy efficiency is estimated by considering electrical energy and input methane energy. The amount of energy needed to convert one cubic meter of methane is

Fig. 10 Reactor operation vs experiment number: *circles*, O_2-to-CH_4 molar ratio 1:5 and feed flow rate 240 mL/min; *stars*, O_2-to-CH_4 molar ratio 1:3 and feed flow rate 134 mL/min; *triangles*, O_2-to-CH_4 molar ratio 1:2 and feed flow rate 225 mL/min. **a** Methane conversion, **b** oxygen conversion
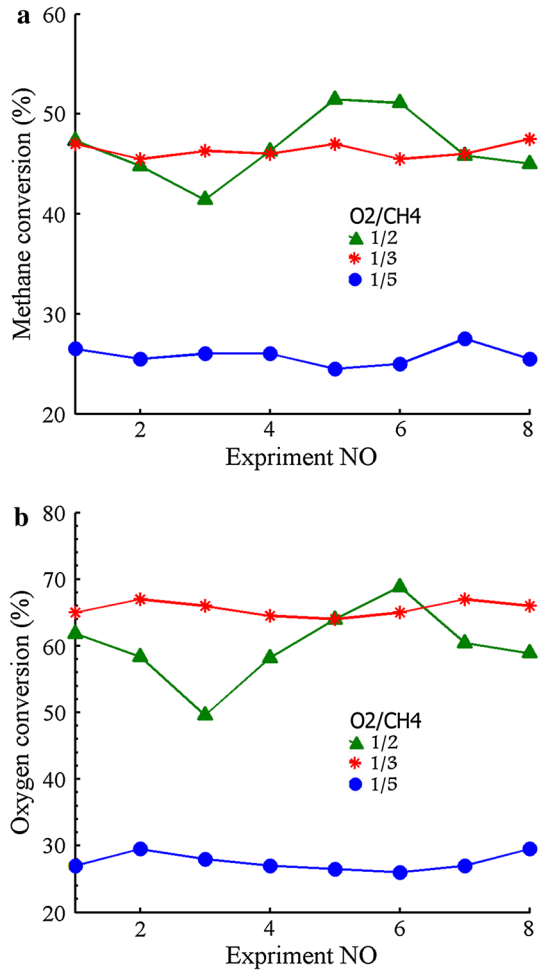
characteristic of the energy cost. On the basis of the range of experiments performed in this study, it can be stated that increasing both the O_2-to-CH_4 molar ratio and the feed flow rate increases energy efficiency and reduces energy cost. This implies that this plasma reactor will become more efficient at large scale, although optimizing energy efficiency was not the purpose of this study. The specific energy density, SED, is defined as the ratio of total input power to feed flow rate. Table 1 shows that, for each O_2-to-CH_4 molar ratio, increasing feed flow rate results in a slow decrease of SED. Higher SED is equivalent to higher release of energy, which results in an increase of the temperature, as already mentioned. In Table 2, the energy efficiency in this study is compared with that for with some well known plasma reactors [28]. According to Table 2, the reactor proposed by Fridman et al. has the highest energy efficiency but, as the authors reported, the gliding arc in a tornado plasmatron has not been designed to manage soot formation. The feed flow should be strong enough to force the arc to move along the electrodes. The RGE

Table 1 Stoichiometry of the reactions for different feed flow rates and compositions

Flow rate (mL/min)		O_2-to-CH_4 molar ratio	Yield (%)		η (%)	Energy cost (kW h/m³)	SED (kJ/L)	α (%)	β (%)	γ (%)	Stoichiometry
In	Out		H_2	CO							
60	85.7	0.2	50.3	19.8	29.42	11.9	50.5	64.3	35.6	7.9	$CH_4 + 0.25O_2 \rightarrow 0.64C + 1.84H_2 + 0.35CO + 0.15H_2O$
120	142.8	0.2	27.5	11	29.13	9.6	40.5	67.1	31.9	16.3	$CH_4 + 0.32O_2 \rightarrow 0.67C + 1.65H_2 + 0.31CO + 0.32H_2O$
180	224.7	0.2	29.6	11.4	38.34	6.7	37.1	65.2	34.7	8.8	$CH_4 + 0.26O_2 \rightarrow 0.65C + 1.82H_2 + 0.34CO + 0.17H_2O$
240	289	0.2	23.6	8.3	39.01	6.3	35.5	67.8	32.1	6.2	$CH_4 + 0.22O_2 \rightarrow 0.67C + 1.87H_2 + 0.32CO + 0.12H_2O$
62.5	85	0.25	45	20.4	27.6	12.6	48.5	58.4	38.9	11.1	$CH_4 + 0.32O_2 \rightarrow 0.58C + 1.73H_2 + 0.38CO + 0.21H_2O$
125	150.7	0.25	29	13.3	31.6	9.7	38.9	63.1	36.8	19.8	$CH_4 + 0.34O_2 \rightarrow 0.63C + 1.6H_2 + 0.36CO + 0.39H_2O$
187.5	218.1	0.25	25.1	11.2	34	6.9	35.7	59.9	40	11.1	$CH_4 + 0.35O_2 \rightarrow 0.59C + 1.77H_2 + 0.4CO + 0.22H_2O$
250	284.3	0.25	24.9	10.7	37.6	5.2	34.1	65.8	34	20.8	$CH_4 + 0.37O_2 \rightarrow 0.65C + 1.58H_2 + 0.34CO + 0.41H_2O$
66.66	85.4	0.33	41.2	26.3	27.8	13.3	45.4	46.7	52.6	16.8	$CH_4 + 0.43O_2 \rightarrow 0.46C + 1.65H_2 + 0.52CO + 0.33H_2O$
133.3	158.3	0.33	35.4	22.3	34.9	7.1	36.4	51.7	48.1	23.3	$CH_4 + 0.47O_2 \rightarrow 0.51C + 1.53H_2 + 0.48CO + 0.46H_2O$
200	227.2	0.33	28.6	17.4	36.3	5.6	33.4	53.9	44.5	24.6	$CH_4 + 0.47O_2 \rightarrow 0.53C + 1.48H_2 + 0.44CO + 0.48H_2O$
266.6	306.1	0.33	26.9	15.8	39.9	4.6	31.9	53.9	44.3	21.4	$CH_4 + 0.44O_2 \rightarrow 0.53C + 1.54H_2 + 0.44CO + 0.42H_2O$
75	89.2	0.5	34.4	32.5	26.9	14.5	40.4	28.1	71.1	24.2	$CH_4 + 0.6O_2 \rightarrow 0.28C + 1.5H_2 + 0.71CO + 0.48H_2O$
150	173.4	0.5	33.8	31	36.6	7	32.4	33	65.9	27.6	$CH_4 + 0.61O_2 \rightarrow 0.33C + 1.43H_2 + 0.65CO + 0.54H_2O$
225	250	0.5	31.7	30.5	40.4	4.6	29.7	34.3	64.5	32.2	$CH_4 + 0.65O_2 \rightarrow 0.34C + 1.33H_2 + 0.64CO + 0.63H_2O$
300	324.3	0.5	25.6	23.1	40.1	4.3	28.4	37.5	59.6	32.5	$CH_4 + 0.64O_2 \rightarrow 0.37C + 1.31H_2 + 0.59CO + 0.63H_2O$

Energy cost kW h/m³ of converted methane

SED, ratio of total input energy to feed flow rate

Table 2 Comparison of the RGE plasma reactor with some well known plasma reactors

Ref.	Reactor	Fuel	Fuel injected (kW)	Reforming process	Plasma power (W)	Efficiency (%)
Bromberg et al. [34]	GEN 2	Methane	11	ATR + catalyst	210	63.5
	GEN 3	Methane	22.5	POX	375	36.7
Fridman et al. [20]	Gliding arc	Methane	1.52	POX	50	75.8
	GAT	Methane	–	POX	200	74
Khacef et al. [35, 36]	Sliding discharge	Methane	2.6	ATR	830	24.5
		Methane	4.6	POX	75	27.5
This study	RGE plasma reactor	Methane	0.046	POX	20	40.1

GEN 2, low-current plasma reactor in which fuels and oxidants are injected near the electrode gap and the cathode can be a spark plug

GEN 3, wide electrode area, low-current plasma reactor in which the species can be injected at different inputs and electrodes are concentric with an axial gap

GAT, gliding arc in tornado plasma reactor

RGE, rotating ground electrode plasma reactor

Table 3 Effect of using air instead of pure oxygen for two flow rates (nitrogen free), 60 mL/min and 120 mL/min. The O_2-to-CH_4 molar ratio was 1:5

Flow rate (mL/min)	Conversion (%)		Selectivity (%)		Byproducts		H-to-CO molar ratio
	Methane	Oxygen	H_2	CO	C (mg/min)	H_2O (mL/min) $\times 10^{-3}$	
60 Using air	62.87	99	80.9	32.2	10.47	8.3	5.01
60 Using oxygen	55	71.2	90.5	35.6	8.8	3.1	5.07
120 Using air	53.2	99	73.4	29.8	18.36	19.8	4.92
120 Using oxygen	34.49	56	79.9	31.9	11.38	7.8	5

plasma reactor operates quite stably in a wide range of feed flows and compositions. The stable discharge which is maintained in this study is of paramount importance, but further attempts should be made to optimize the energy efficiency of the RGE plasma reactor.

Using air instead of pure oxygen

When electrons collide with molecules, electronic excitation and dissociation of the molecules into atoms can occur. Because no nitrogen compounds except nitrogen itself were present in the products (GC analysis showed no unknown peak), we propose excitation of the nitrogen molecules in this study. As reported by Savinov et al. [33], the dissociation energy of nitrogen molecules is almost twice that of methane molecules. Therefore nitrogen molecules are easily excited to high vibrational levels and will act as a source of energy for activation of reagent

molecules in the reactor. It is evident from Table 3 that use of air instead of pure oxygen promotes the conversion of methane and oxygen. This is because the methane and oxygen molecules are being activated to react with each other, because of the presence of excited nitrogen molecules. It is also apparent from Table 3 that using air instead of pure oxygen increases the production of byproducts, thus reducing selectivity for hydrogen and carbon monoxide. This is because of a sharper increase in conversion of oxygen compared with conversion of methane when air is used. Also note that an excited molecule of nitrogen can activate only gaseous reagents and has no effect on solid carbon.

Conclusions

Electron collisions and methane partial oxidation reactions are responsible for the partial oxidation of methane occurring in this reactor to produce syngas. A wide range of H_2-to-CO (syngas) molar ratios could be produced by use of this reactor. Increasing the O_2-to-CH_4 molar ratio promotes further methane partial oxidation reactions at higher feed flow rates. At some O_2-to-CH_4 molar ratios, increasing the feed flow rate to a specific value promotes conversion of the reagents. Although selectivity for carbon monoxide increases, that for hydrogen decreases when the O_2-to-CH_4 molar ratio is increased. In this study, energy efficiency was approximately 40 % under stable conditions despite soot formation, which is inevitable when syngas is produced by partial oxidation of methane. The products are carbon, hydrogen, carbon monoxide, and water. Competing reactions produce hydrogen and water; the same is true for carbon and carbon monoxide.

References

1. Z. Gu, K. Li, H. Wang, Y. Wei, D. Yan, T. Qiao, Kinet. Catal. **54**(3), 326 (2013)
2. H. Liu, D. He, Catal. Surv. Asia **16**(2), 53 (2012)
3. H. Özdemir, M. Öksüzömer, M.A. Gürkaynak, Fuel **116**, 63 (2013)
4. J. Yuan, L. Liu, L. Wang, C. Hao, Catal. Lett. **143**(1), 126 (2013)
5. Y. Song, H. Liu, S. Liu, D. He, Energy Fuels **23**(4), 1925 (2009)
6. J.E.P. Navalho, I. Frenzel, A. Loukou, J.M.C. Pereira, D. Trimis, J. Pereira, Int. J. Hydrog. Energy **38**(17), 6989 (2013)
7. S. Cimino, L. Lisi, Ind. Eng. Chem. Res **51**(22), 7459 (2012)
8. S.S. Kim, J. Kim, H. Lee, B.K. Na, H.K. Song, Korean J. Chem. Eng. **22**(4), 585 (2005)
9. F. Odeyemi, M. Pekker, A. Rabinovich, A.A. Fridman, M. Heon, V.N. Mochalin, Y. Gogotsi, IEEE Trans. Plasma Sci. **40**(5), 1362 (2012)
10. K. Pornmai, A. Jindanin, H. Sekiguchi, S. Chavadej, Plasma Chem. Plasma Process **32**(4), 723 (2012)
11. M. Badani, J. Huang, S. Suib, J. Harrison, M. Kablauoi, Res. Chem. Intermed. **21**(6), 621 (1995)
12. S.L. Brock, T. Shimojo, S.L. Suib, Y. Hayashi, H. Matsumoto, Res. Chem. Intermed. **28**(1), 13 (2002)
13. W. Cho, Y. Baek, Y.C. Kim, M. Anpo, Res. Chem. Intermed. **28**(4), 343 (2002)
14. W. Cho, Y. Baek, D. Park, Y.C. Kim, M. Anpo, Res. Chem. Intermed. **24**(1), 55 (1998)
15. J. Huang, S. Suib, J.B. Harrison, F. Knight, Res. Chem. Intermed. **27**(6), 643 (2001)
16. L. Bromberg, D. Cohn, A. Rabinovich, C. O'Brie, S. Hochgreb, Energy Fuels **12**(1), 11 (1998)
17. M. Rafiq, J. Hustad, Ind. Eng. Chem. Res. **50**(9), 5428 (2011)

18. T. Sreethawong, P. Thakonpatthanakun, S. Chavadej, Int. J. Hydrog. Energy **32**(8), 1067 (2007)
19. K. Supat, A. Kruapong, S. Chavadej, L.L. Lobban, R.G. Mallinson, Energy Fuels **17**(2), 474 (2003)
20. C.S. Kalra, A.F. Gutsol, A.A. Fridman, IEEE Trans. Plasma Sci. **33**(1), 32 (2005)
21. M. Moshrefi, F. Rashidi, H. Bozorgzadeh, M.E. Haghighi, Plasma Chem. Plasma Process **33**(2), 453 (2013)
22. M.M. Moshrefi, F. Rashidi, H.R. Bozorgzadeh, S.M. Zekordi, Plasma Chem. Plasma Process **32**(6), 1157 (2012)
23. M.M. Moshrefi, F. Rashidi, J. Nat. Gas Sci. Eng **16**, 85 (2014)
24. R.A. Serway, *Principles of Physics*, 2nd edn. (Brooks/Cole, Pacific Grove, 1998)
25. H.J. Gallon, X. Tu, M.V. Twigg, J.C. Whitehead, Appl. Catal. B **106**(3), 616 (2011)
26. D. Li, X. Li, M. Bai, X. Tao, S. Shang, X. Dai, Y. Yin, Int. J. Hydrog. Energy **34**(1), 308 (2009)
27. L.A. Arkatova, O.V. Pakhnutov, A.N. Shmakov, Y.S. Naiborodenko, N.G. Kasatsky, Catal. Today **171**(1), 156 (2011)
28. G. Petitpas, J.-D. Rollier, A. Darmon, J. Gonzalez-Aguilar, R. Metkemeijer, L. Fulcheri, Int. J. Hydrog. Energy **32**(14), 2848 (2007)
29. M.H. Rafiq, H.A. Jakobsen, J.E. Hustad, Fuel Process. Technol. **101**, 44 (2012)
30. D.H. Lee, K.T. Kim, Y.H. Song, W.S. Kang, S. Jo, Plasma Chem. Plasma Process **33**(1), 249 (2012)
31. W. Sun, M. Uddi, S.H. Won, T. Ombrello, C. Carter, Y. Ju, Combust. Flame **159**(1), 221 (2012)
32. M. Deminskii, I. Chernysheva, S.Y. Umanskii, M. Strelkova, A. Baranov, I. Kochetov, A. Napartovich, T. Sommerer, S. Saddoughi, J. Herbon, Russian j. Phys. Chem. B **7**(4), 410 (2013)
33. S.Y. Savinov, H. Lee, H.K. Song, B.-K. Na, Plasma Chem. Plasma Process. **23**(1), 159 (2003)
34. L. Bromberg, D.R. Cohn, A. Rabinovich, N. Alexeev, A.V. Samokhin, K. Hadidi, J.E. Palaia, N.M. Bel, *Onboard plasmatron hydrogen production for improved vehicles* (Plasma Science and Fusion Center, Massachusetts Institute of Technology, Cambridge, 2006)
35. E.E. Ahmar, C. Met, O. Aubry, A. Khacef, J. Cormier, Chem. Eng. J. **116**(1), 13 (2006)
36. F. Ouni, A. Khacef, J.M. Cormier, Chem. Eng. Technol. **29**(5), 604 (2006)